THE IJES

Fluid flow and heat transfer across a circular cylinder in the unsteady flow regime

Ravi Golani[1*] and A. K. Dhiman[2]

[1]*Tata Steel limited, India 831001*
[2]*Department of Chemical Engineering, IIT Roorkee, India 247667*

---**ABSTRACT**---

Fluid flow past an obstacle of circular cross-section represents a classical fluid mechanics problem and has received much attention for over a century or so. In the present study, the fluid flow and heat transfer from a two-dimensional circular cylinder is considered in the unsteady flow regime. In particular, the effect of Reynolds number on on drag and lift coefficients, Strouhal number and the heat transfer characteristic of a long circular cylinder (heated) are investigated for Reynolds number range: Re = 50-180 (in the steps of 10) and Prandtl number = 0.7 (air) in the unconfined unsteady cross-flow. The numerical simulations have been carried out by using finite volume method (FVM) based commercial CFD solver Fluent (version 6.3). Detailed flow patterns are presented by way of instantaneous streamline, vorticity magnitude, velocity magnitude and pressure contours. The present results are found to be in an excellent agreement with the experimental/numerical data available for a circular cylinder in the literature. Heat transfer results are presented here by the variation of Nusselt number with time as well as by isotherm profiles for the above range of conditions. The average Nusselt number increases with increasing Reynolds number. As the Reynolds number increases, the drag coefficient and shedding frequency increases, however, the rms drag and rms lift coefficients increase with Reynolds number. Finally, simple correlation for time-averaged drag coefficient and time average Nusselt number as a function of Reynolds number are obtained for the range of conditions covered in this study.

Keywords: *Circular cylinder; unsteady regime; Reynolds number; Nusselt number.*

Date of Submission: 15 March 2014   Date of Publication: 30 March 2014

I.   INTRODUCTION

Owing to its theoretical and numerical importance, the problem of viscous incompressible fluid flow and forced convection heat transfer past a long cylinder of circular cross-section has been topic of intense study for a century or so. The problem under consideration has also a model for fundamental studies of challenging fluid mechanics problems, as well as representing an important class of engineering applications such as tubular and plate-fin type heat exchangers, cooling towers, hot wire anemometer, nuclear reactor fuel rods, cable-stayed and suspension bridges, offshore risers, sensors and probes, etc. Excellent reviews, survey articles and even entire books are available for the fluid flow over these long cylinders of circular cross-section (Ahmad, 1996; Lange et al., 1998; Norberg, 2003; Zdravkovich, 1997, 2003, etc.).

Williamson (1988) stated that the flow past a circular cylinder undergoes several interesting changes with Reynolds number. A universal and continuous Strouhal-Reynolds number relationship for the laminar vortex shedding of a circular cylinder for the Reynolds number range of 49 to 178 has been presented. He concluded that if careful attention was paid to the damping of any circular cylinder vibrations and if the stream was sufficiently uniform, the Strouhal curves for parallel shedding should be completely smooth and devoid of discontinuities. The characteristics of the flow past a circular cylinder change with Reynolds number according to the following regimes: occurrence of vortex shedding at Re = 50 and wake transition at Re = 180. Baranyi (2003) did computations of the unsteady momentum and heat transfer for a fixed circular cylinder in the laminar flow regime for the Reynolds number range from 50 to 180. The finite difference method has been employed to solve the Navier-Stokes and Poisson equations. The diameter of the outer boundary of computation is 30 times larger than the diameter of the cylinder and O type grid is used. Drag and lift coefficients and also Strouhal number variations with the Reynolds number are computed and found that they had a good agreement with the experimental results, even the 3-D wake formation at about Re = 160. Posdziech and Grundmann (2007) performed 2-D numerical simulations of the flow around the cylinder for Re = 5 to 250 by using spectral element method. They have shown that the unsteady drag variation was smaller compared to the steady case and the lift coefficient strongly increased with Reynolds number. The Reynolds number dependency on drag, lift and

base pressure coefficients and Strouhal-Reynolds relationship were given polynomial approximations up to fifth order. From the intersection of steady and unsteady Reynolds number relationships, the critical Reynolds number of the primary instability was determined as Re = 46.7. Recently, Rajani et al. (2008) have studied numerically the laminar flow past a circular cylinder for Re = 100 to 400. An implicit pressure-based finite volume method was used here. The temporal evolution of the lift and drag coefficients have been computed separately from both 2-D and 3-D simulations of the flow for the values of Re = 100, 200, 250, 300 and 400. They also reported that up to Re = 200, 2-D and 3-D computation results are observed to be almost overlapping, showing no significant difference in the temporal variation of the lift and drag coefficients at the statistically stationary state. Nakamura and Igarashi (2004) experimentally investigated the change in the heat transfer according to flow regimes, namely, laminar shedding, wake transition and shear layer transition regimes for the Reynolds number range 70 – 30000. The Nusselt number at the rear stagnation point increases with Reynolds number in the laminar shedding regime for Re <150. Shi et al. (2004) investigated the effect of temperature dependent viscosity and density of air on the fluid flow and heat transfer from a heated cylinder for the range$10^{-3} \le$ Re $\le$170. Isaev et al. (2005) has used two-dimensional Navier–Stokes and energy equations to carry out the numerical calculation of the parameters of unsteady state flow and heat transfer under conditions of laminar transverse flow of a viscous incompressible fluid past a circular cylinder for the fixed value of the Reynolds number of 140. The calculation results have revealed that a process of cyclic heating of the wake is observed under these conditions, with the formation of a temperature street similar to Karman vortex street. Mahir et al (2008) has investigated the unsteady laminar convective heat transfer from isothermal cylinders of tandem arrangement. The analysis is carried out for the Reynolds numbers of 100 and 200 and for centre-to-centre distance ratio of 2, 3, 4, 5, 7 and 10. The mean and local Nusselt numbers for the upstream and downstream cylinders were obtained. It is found that the mean Nusselt number of the upstream cylinder approaches to that of a single isothermal cylinder for the centre-to-centre distance ratio greater than 4 and the mean Nusselt number of the downstream cylinder is about 80% of the upstream cylinder.

Thus, based upon the above discussion, it can be summarized here that wealth of information is available in the open literature on the value of the critical Reynolds number and the flow parameters such as drag, lift and Strouhal number for the fluid flow past an obstacle of circular cross-section in the unsteady (periodic) cross-flow regime. However, limited information is available on the pressure, velocity and vorticity fields and heat transfer characteristics around the cylinder in unsteady periodic flow regime. Therefore, the objective of this study is to carry out the numerical calculations for the Reynolds number 50-180 (in the steps of 10) for the air like fluids.

II.   PROBLEM STATEMENT AND MATHEMATICAL FORMULATION

In the present study, the two-dimensional unsteady flow of an incompressible fluid (with a uniform velocity (U_∞) and temperature (T_∞) at the inlet) across a circular cylinder is considered as shown in Figure 1. The surface of the cylinder is maintained at a constant temperature, T_w^* ($> T_\infty$). The thermo-physical properties of the streaming fluid are assumed to be independent of the temperature and the viscous dissipation effects are also neglected. The temperature difference between the surface of the cylinder and the streaming liquid is assumed to be small so that the variation of the physical properties, notably, density and viscosity, with temperature could be neglected. The unconfined flow condition is simulated by creating an artificial circular boundary of diameter D_∞. The outer boundary ($D_\infty = 300d$) is taken to be sufficiently large such that the end effects are negligible.
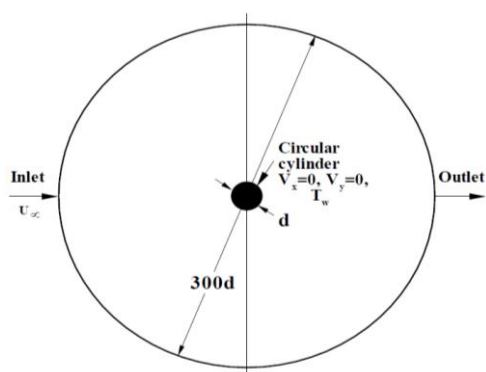

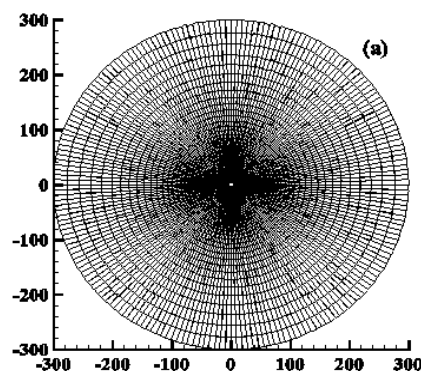Fig 1: Schematic of flow around the circular cylinder   Fig 2: Non-uniform computational grid structure

The governing equations (in their dimensionless forms) are the continuity, the x- and y-components of the Navier–Stokes equations and energy equation, which are presented by equations (1) - (4). The Reynolds number is defined as $Re = dU_\infty\rho/\mu$, where μ and ρ are the viscosity and the density of working fluid, respectively.

Continuity Equation:

$$\frac{\partial V_x}{\partial x} + \frac{\partial V_y}{\partial y} = 0 \qquad (1)$$

x-Momentum equation:

$$\frac{\partial V_x}{\partial t} + \frac{\partial\left(V_x V_x\right)}{\partial x} + \frac{\partial\left(V_y V_x\right)}{\partial y} = -\frac{\partial p}{\partial x} + \frac{1}{Re}\left(\frac{\partial^2 V_x}{\partial x^2} + \frac{\partial^2 V_x}{\partial y^2}\right) \qquad (2)$$

y-Momentum equation:

$$\frac{\partial V_y}{\partial t} + \frac{\partial\left(V_x V_y\right)}{\partial x} + \frac{\partial\left(V_y V_y\right)}{\partial y} = -\frac{\partial p}{\partial y} + \frac{1}{Re}\left(\frac{\partial^2 V_y}{\partial x^2} + \frac{\partial^2 V_y}{\partial y^2}\right) \qquad (3)$$

Energy equation

$$\frac{\partial T}{\partial t} + \frac{\partial(V_x T)}{\partial x} + \frac{\partial(V_y T)}{\partial y} = \frac{1}{Pe}\left(\frac{\partial^2 T}{\partial x^2} + \frac{\partial^2 T}{\partial y^2}\right) \qquad (4)$$

The physical realistic dimensionless boundary conditions for the fluid flow around an unconfined cylinder may be written as follows (Figure 1):

- At the inlet: The condition of uniform flow is used, i.e., $V_x=1$, $V_y=0$ and $T=0$.
- On the cylinder surface: No-slip condition of velocity is used, i.e., $V_x=0$, $V_y=0$ and $T=1$.
- At the exit boundary: The default outflow boundary condition in FLUENT, which assumes a zero diffusion flux for all flow variables, is used. Physically, this condition implies that the conditions of the outflow plane are extrapolated within the domain and have negligible impact on the upstream flow conditions. This is similar to Neumann boundary condition as $\partial V_x/\partial x = 0$, $\partial V_y/\partial x = 0$ and $\partial T/\partial x = 0$.

The governing equations (1) – (4) along with above noted boundary conditions are solved for the fluid flow and heat transfer over a long circular obstacle to obtain velocity, pressure and temperature fields, which can be utilized to calculate the engineering parameters such as drag and lift coefficients and the Shrouhal number and Nusselt number, etc.

- Drag coefficient: The total drag coefficient on any body consists of two components, e.g., skin friction drag (C_{DF}) and form drag (C_{DP}) coefficients. The skin friction drag is a result of the viscous forces acting on the body while the form drag is due to the unbalanced pressure forces on the body. The total drag coefficient can be calculated as $C_D = C_{DF} + C_{DP}$.

- Lift coefficient: Similar to total drag coefficient, total lift coefficient on any body consists of friction lift (C_{LF}) and pressure lift (C_{LP}) coefficients and can be calculated as $C_L = C_{LF} + C_{LP}$.

- In the unsteady periodic flow regime, vortices are shed by the bluff body from one side, then from the other and the most frequently used flow quantity is the non-dimensional frequency of vortex shedding and defined as $St = fd/U_\infty$, where St is the Strouhal number, f is the vortex shedding frequency, d is the diameter of cylinder and U_∞ is the free stream velocity, respectively.

- Nusselt number: In this study, the local Nusselt number (Nu) is defined as $-\partial T/\partial n$, where n is the cylinder surface normal direction. The average Nusselt number is calculated by averaging the local Nusselt number over the surface of the cylinder. The time averaged Nusselt number is calculated by averaging 10 cycles (beyond the time the asymptotic shedding frequency of the Karman vortex is attained).

III. NUMERICAL DETAILS

In this study, the O-type grid structure is created by using commercial grid generator GAMBIT. It consists of non-uniform quadrilateral cells having a total of 24000 grid points in the computational domain as shown in Figure 2. The grid near the surface of the cylinder is sufficiently fine to resolve the boundary layer around the cylinder. The nearest grid point from the obstacle is taken to be at a distance of $0.0015d$, where d is the diameter of the cylinder. The outer boundary is taken to be at a distance of $300d$.

The fluid flow over a long circular obstacle is solved by commercial software package FLUENT (6.3) in an unconfined regime. FLUENT uses finite volume method, according to which, it is assumed that volume is made up of large number of small volume elements, which are regular parallelepiped. The governing equations are valid over all such control volumes. Hence, equations can be discretized to be written in algebraic form to be solved. The values at the finite volumes can be summed up to get the value over entire domain. The grid is generated by using GAMBIT. A very fine grid of cell size, $\delta = 0.0015d$ is used near the cylinder and larger size grids are used away from the cylinder. The second order upwind scheme is used to discretize convective terms of momentum equations while the diffusive term is discretized by central difference scheme. The resulting algebraic equations are solved by Gauss-Siedel iterative scheme. A convergence criterion of 10^{-20} is used for continuity, the x- and y-components of the Navier–Stokes equations.

IV. RESULTS AND DISCUSSION

In this study, the numerical simulations of the fluid flow and heat transfer across a long circular cylinder have been carried out for the Reynolds number: Re = 50 to 180 (in the steps of 10). Based upon the information available in the literature (Williamson, 1988; Zdrakovich, 1997, 2003 and others), the flow for the above range of conditions is unsteady and periodic in nature.

4.1 Validation of Results

In order to validate the present numerical solution procedure, numerical computations have been carried out at different values of Reynolds number and tabulated in Tables 1. Table 1 presents the comparison of time-averaged drag coefficient, rms value of the lift coefficient and Shrouhal number at Re = 100. The percentage deviations of present time-averaged drag results are less than 0.30 % with Posdziech and Grundmann (2007), about 1.2 % with Mittal (2005), less than 2.5 % with Rajani et al. (2008). Similarly, the percentage deviations of present Strouhal number results are less than 0.25 % with Posdziech and Grundmann (2007), Baranyi (2003), about 1.1 % with Mittal (2005) and about 3.5 % with Rajani et al. (2008). The comparison of present Nusselt number results with literature values for Reynolds number of 100 can be seen in Table 2. It can be seen that the time averaged Nusselt number is in an excellent agreement with the literature values. For instance, the percentage deviations in the values of the time averaged Nusselt numbers are found to be only about 2.0 %, 0.25 %, 0.9 % and 1.8 % with the results of Knudsen and Katz (1958), Zhuauskas (1972), Baranyi (2003) and Mahir et al. (2008) for the value of the Reynolds number of 100. This validates the present numerical solution procedure. Therefore, it can be summarized here that the present results are in an excellent agreement with all studies and the slight differences between the present values and that of the others are due to the different domain and grid sizes used by others as opposed to the present study.

Table 1: Validation of time-average drag coefficient, rms value of lift coefficient and Strouhal number at Re = 100

Author (literature)	$\bar{C}_D$	C_{Lrms}	St
Present work	1.3063	0.2181	0.1626
Rajani et al. (2008)	1.3353	0.1792	0.1569
Posdziech and Grundmann (2007)	1.31	-	0.163
Mittal (2005)	1.322	0.2256	0.1644

Table 2: Validation of Nusselt number results with Literature Values at Re = 100

Author (literature)	$\overline{Nu}$
Present work	5.0866
Knudsen and Katz (1958)	5.19
Zhuauskas (1972)	5.10
Mahir et al. (2008)	5.179
Baranyi (2003)	5.132

4.2 Flow Patterns

The flow field around the unconfined circular obstacle is presented by way of instantaneous streamline, vorticity magnitude, velocity magnitude and pressure profiles for different values of Reynolds numbers. Figure 3 present the instantaneous streamline; however, Figure 4 show the velocity magnitude contours in the vicinity of the cylinder for Reynolds number of 150 for nine successive moments of time which span over the whole period. Similarly, the instantaneous vorticity magnitude contours have been shown in Figure 5 for the corresponding value of the Reynolds number. These figures clearly show that two vortices are formed and shed from the surface of the cylinder alternatively. The flow gets detach from the surface of the circular obstacle at the separation point and forms a region of slow moving eddies behind the obstacle. In this region, the wake is bounded by a shear layer extending from the separation point on each side of the obstacle. On the other hand, there is faster moving free flow outside of this shear layer. Due to the difference in the flow velocity on either side of the shear layers, these shear layers tend to roll up on themselves forming vortices. Further increase in the velocity, the flow separation point organizes into a line along the obstacle where the shear layers roll into line like vortices extending along the cylinder. Figure 5 also demonstrate the effective transport of energy away from the surface of the cylinder and/or energy convected is bounded tightly inside the vortices. The periodic variations in the wake behind the obstacle can also be seen by the instantaneous pressure contours around the cylinder, as shown in Figure 6. These figure reveal high pressures near the front stagnation region and low pressures behind the cylinder, i.e., in the wake region, which is followed by the periodic formation of low and high pressures in the far downstream of the cylinder.
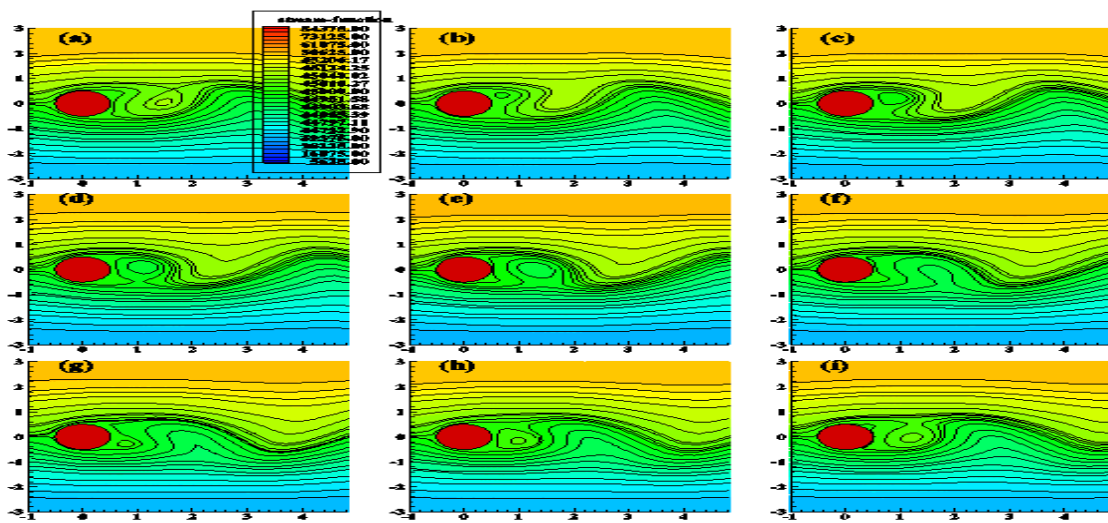

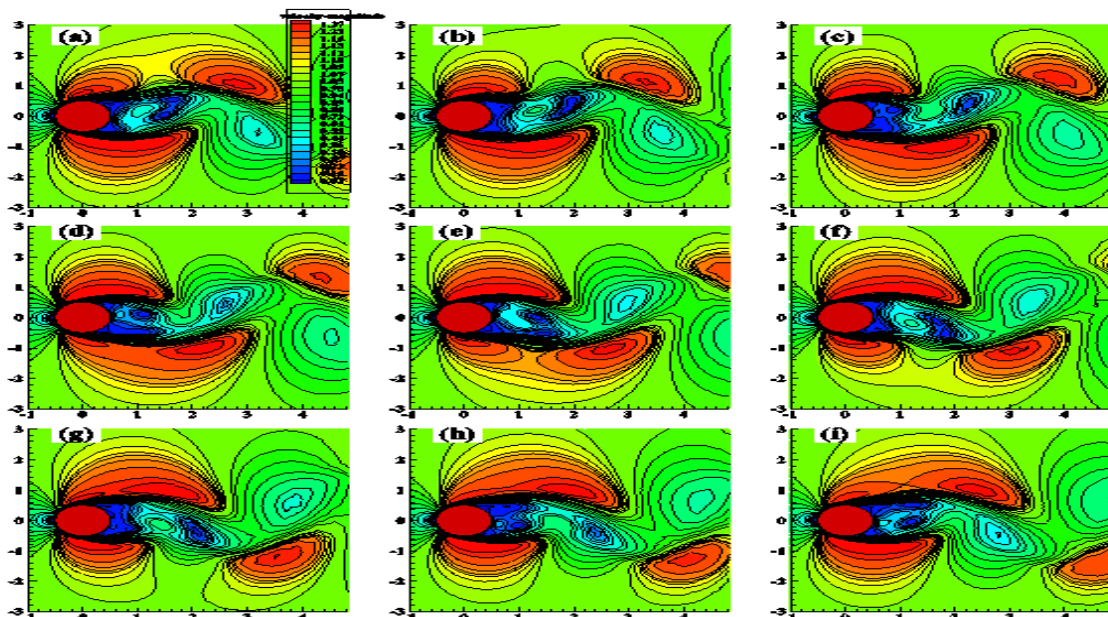Figure 3: Instantaneous streamline profile at Reynolds number of 150.

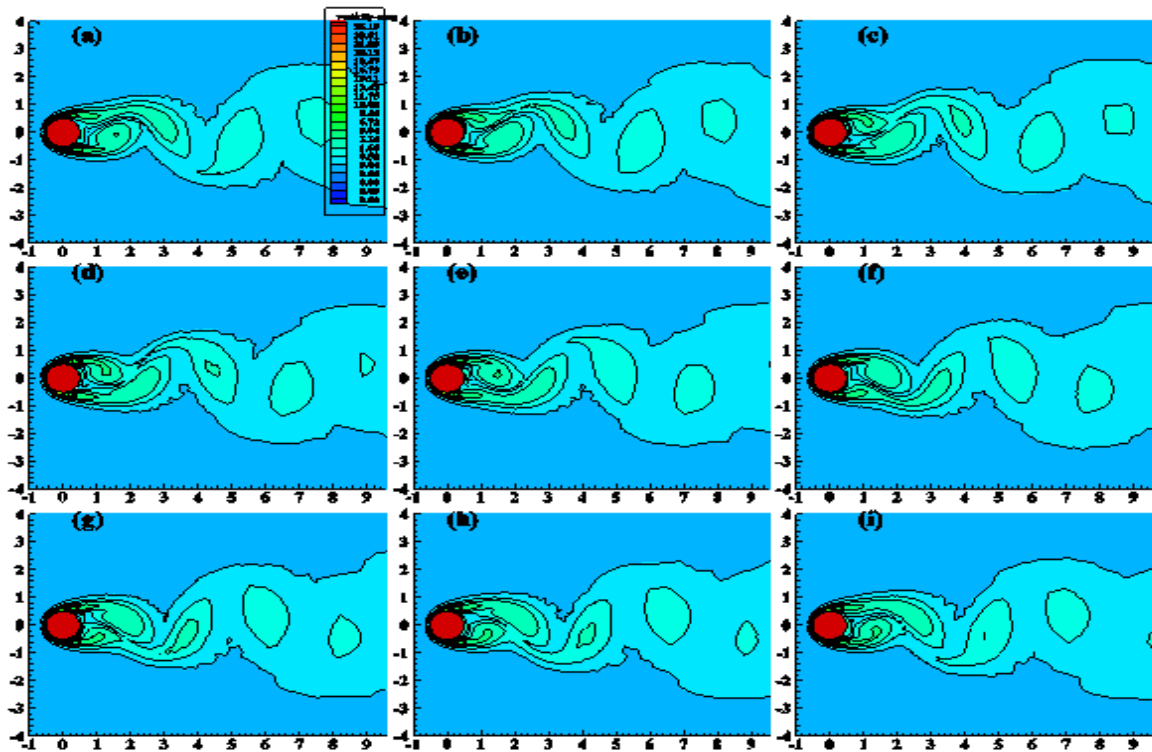Figure 4: Instantaneous velocity magnitude profile at Reynolds number of 150

Figure 5: Instantaneous vorticity magnitude profile at Reynolds number of 150.
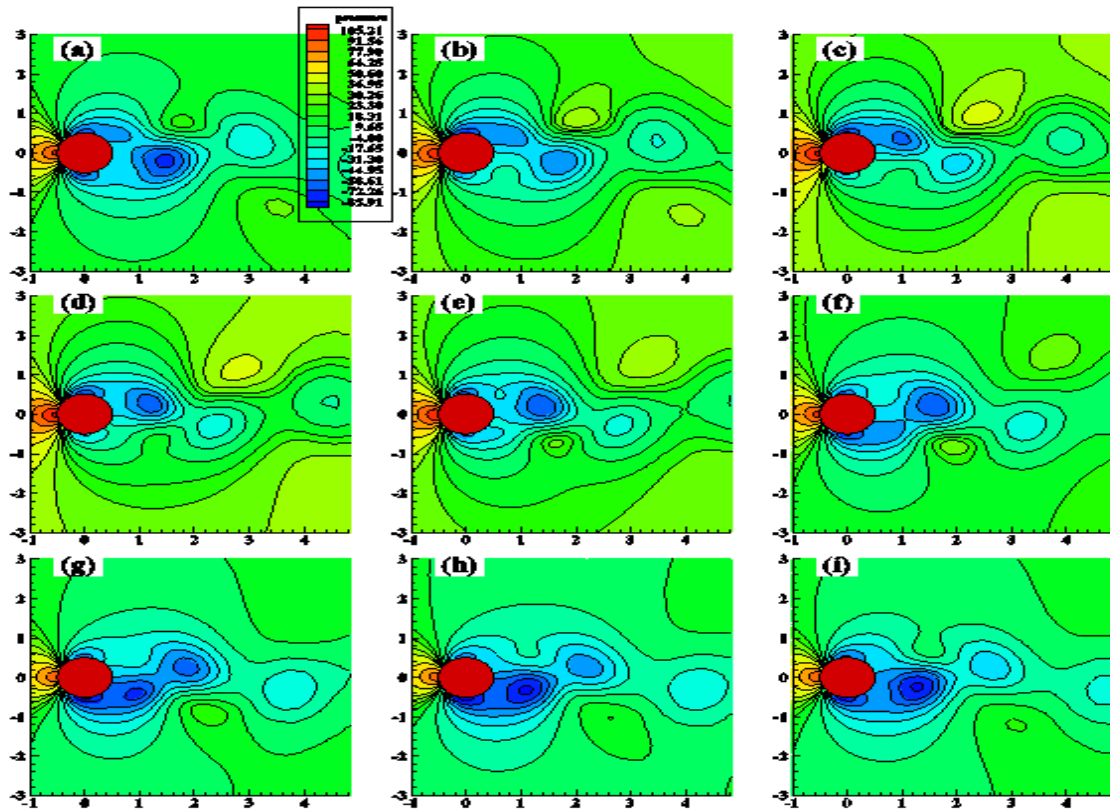

Figure 6: Instantaneous pressure field at Reynolds number of 150.

4.3 Isotherm Patterns

The representative instantaneous isotherms near the cylinder are presented for the Reynolds number of 150 in Figs. 7 (a - e) for five successive moments of time, which span over the whole period. Note that Figure 7 (a) will be repeated after Figure 7 (e) for the next cycle. These figures reveal that a temperature street is formed downstream the cylinder, which is very similar to von Karman Vortex Street for all the values of the Reynolds number covered here. It is also clear from these figures that the front surface of the cylinder has the maximum clustering of isotherms which results in high temperature gradients as compared to the other points on the surface of the cylinder. Since one of the main objectives in heat transfer calculations is to determine the total heat transfer from the isothermal cylinder. The effect of the flow structure especially on heat transfer can be observed by analyzing the heat transfer coefficient of the cylinder. These details are provided in the following subsection.
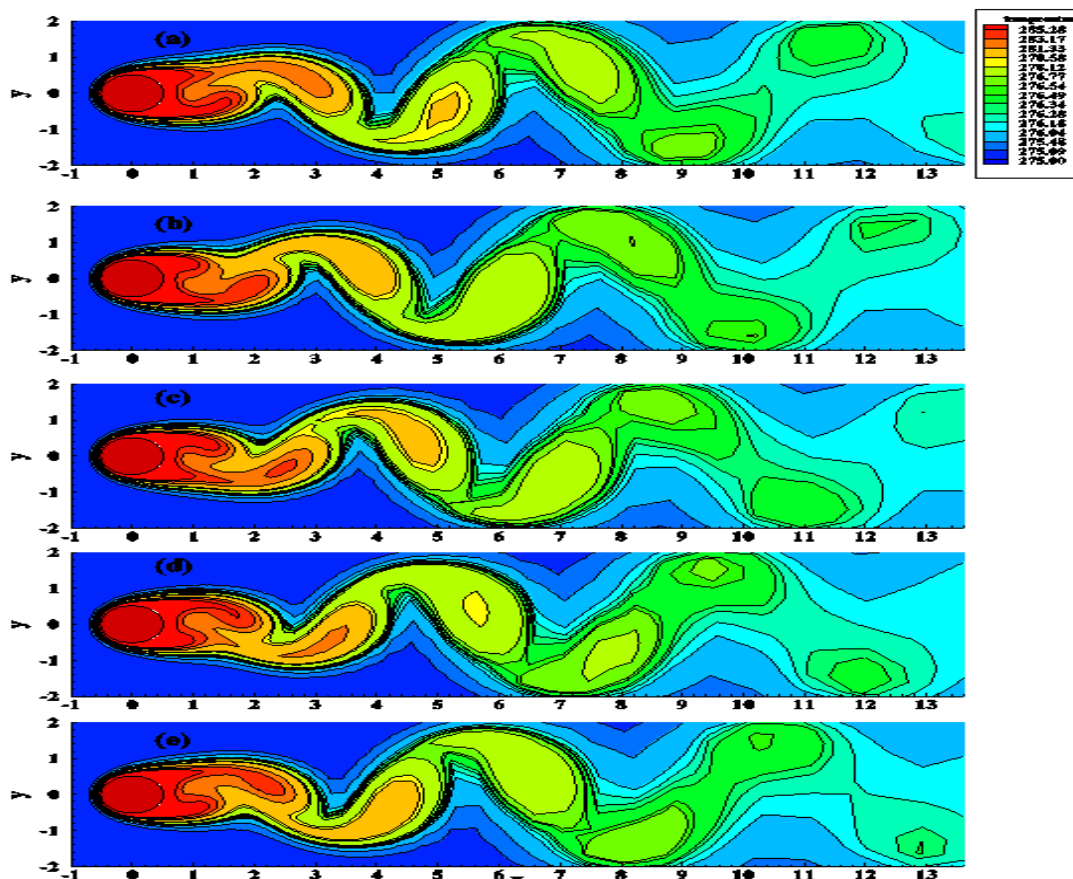

Figure 7: Instantaneous Isotherms for Re = 150

4.4 Drag Coefficient

Fig 8 shows the total drag coefficient history for the values of the Reynolds numbers of 100 and 150. For this, the instantaneous values of the drag coefficient are calculated at each time step and plotted versus time. Initially, the value of the drag coefficient oscillates and finally stabilizes with time for all the cases. The time average drag coefficient is calculated by averaging 20 cycles (beyond the time the asymptotic shedding frequency of the Karman vortex is attained). The variation of the time-averaged drag coefficient with Reynolds number is presented in Figure 9(a). The value of the time-averaged drag coefficient decreases with increasing value of the Reynolds number. Likewise, the variation of the rms value of the drag coefficient with Reynolds number is shown in Figure 9(b).The value of the time-averaged drag coefficient decreases with increasing value of the Reynolds number (Table 3). Further, these drag values have been utilized in order to obtain the simple correlation for the time-averaged drag coefficient. Equation (4.1) presents the simple correlation for the time-averaged drag coefficient.

$$C_D = 1.2254 + 0.8189\,\mathrm{Re}^{-0.4464}$$

(5.1)

This expression, i.e., Eq. (5.1) has a maximum deviation of about 2 % as compared to the present computed results for the range of Reynolds number 50 – 180.
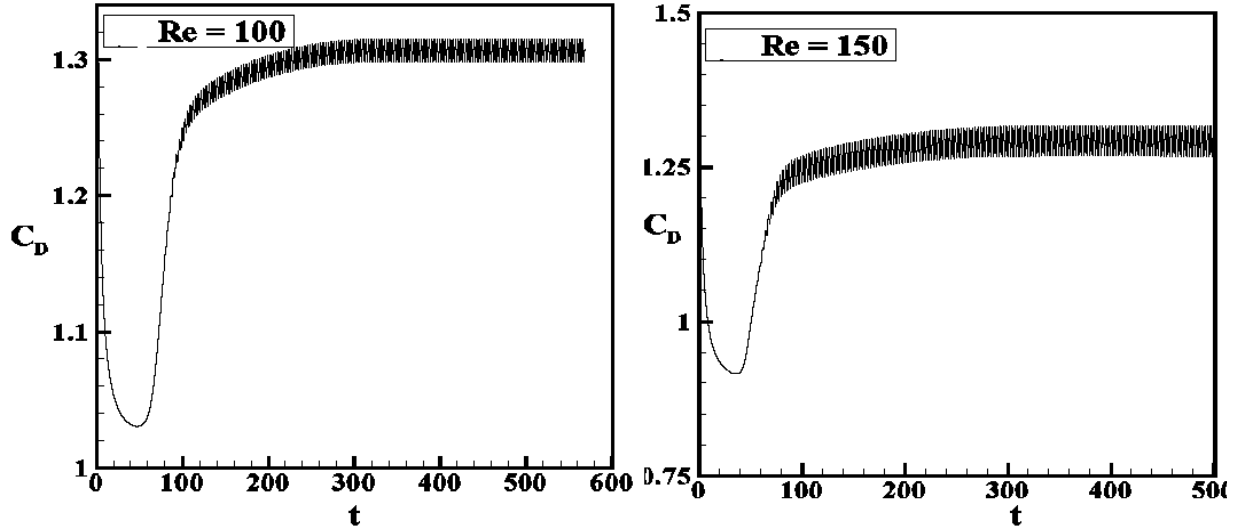

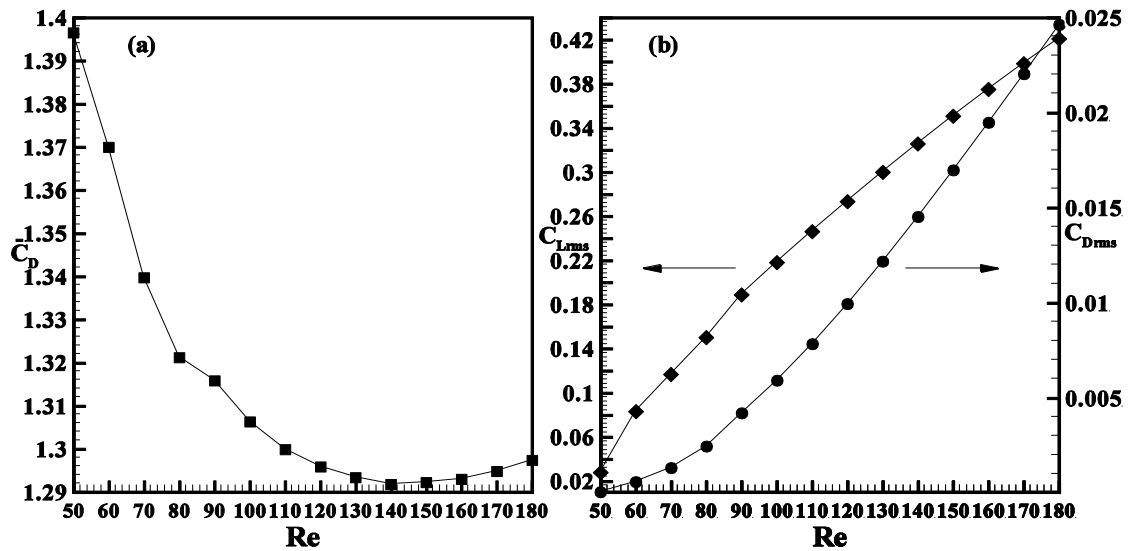Figure 8: Time history of total drag coefficient for Re = 100 and 150

Figure 9: Variation of (a) time-averaged drag coefficient and (b) rms value of drag and lift coefficients with Reynolds number.

4.4 Lift Coefficient
      Similar to drag results, the variation of the lift coefficient with time for the Reynolds number range: Re = 100 and 150 is shown in Figure 10. The value of the lift coefficient initially oscillates and finally stabilizes with time for all the values of the Reynolds number. The variation of the rms value of the lift coefficient with Reynolds number is also shown in Figure 9(b). The rms lift coefficient increases monotonically as the Reynolds number increases. Note that the magnitude of the rms lift coefficient is one order higher than that of the rms drag coefficient. It is found that the time-averaged lift coefficient remains approximately zero for all the values of the Reynolds number considered here.
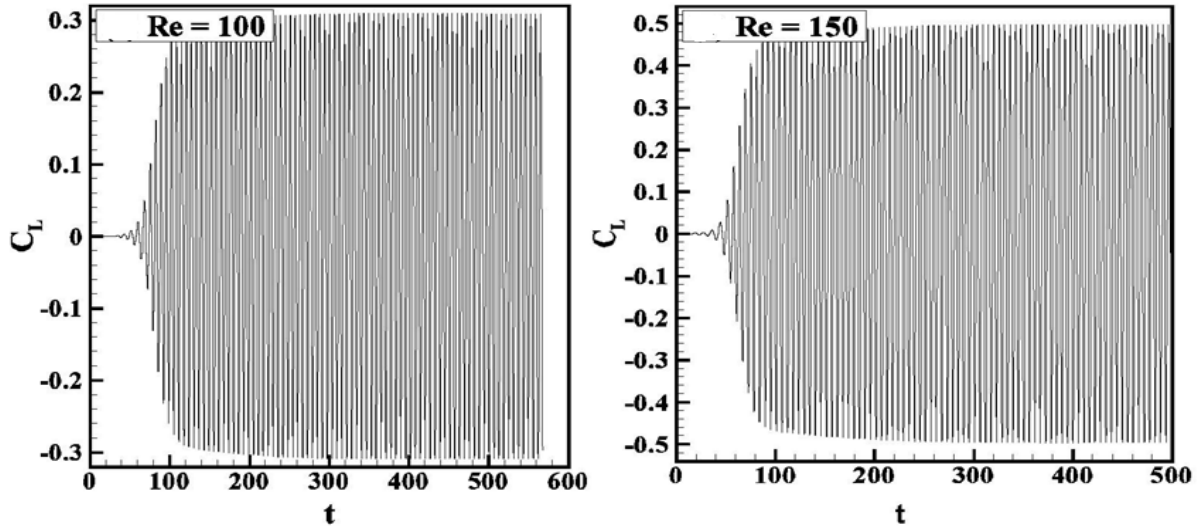
Figure 10: Time history of total lift coefficient for Re = 100 and 150

4.5 Nusselt number

Figures 11 show the time history of Nusselt number for the values of the Reynolds numbers of 100 and 150. Initially, the value of the Nusselt number oscillates and finally stabilizes with time for all the cases considered here. The time averaged Nusselt number is calculated by averaging 10 cycles (beyond the time the asymptotic shedding frequency of the Karman vortex is attained). The time averaged values of the Nusselt number are presented in Table 3. The time averaged Nusselt number increases with increasing value of the Reynolds number for the Prandtl number of 0.7 as shown in Figure 12. We have developed a correlation between these parameters based on our numerical study for the range 50≤Re≤180.

The following simple expressions of average Nusselt number can be used in order to calculate the intermediate values of the time-average Nusselt number within the range of 50 ≤Re ≤180.

$$\overline{Nu} = 0.5650 \times Pr^{1/3} \times Re^{0.5050} \qquad (5.2)$$

Equation (5.2) has a maximum deviation of less than 1.3 % with the computed values of the Nusselt number.

Table 3: Time-averaged drag coefficient, rms value of drag and lift coefficients and Nusselt number with Reynolds number.

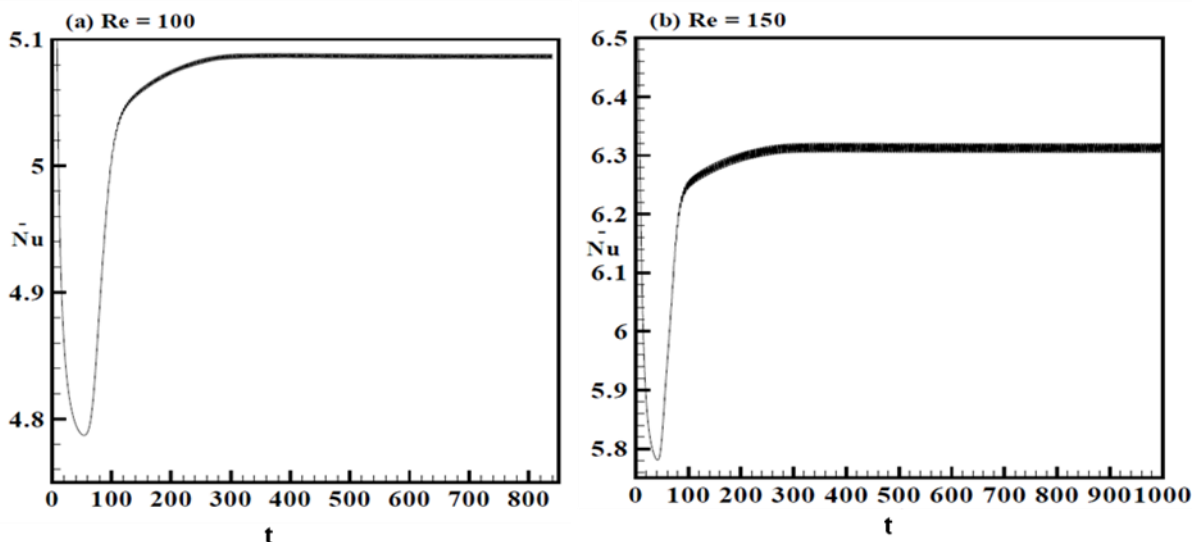| Re	$\overline{C_D}$	C_{Lrms}	C_{Drms}	$\overline{Nu}$
100	1.3063	0.2181	0.0065	5.0866
150	1.2923	0.3508	0.0157	6.3126

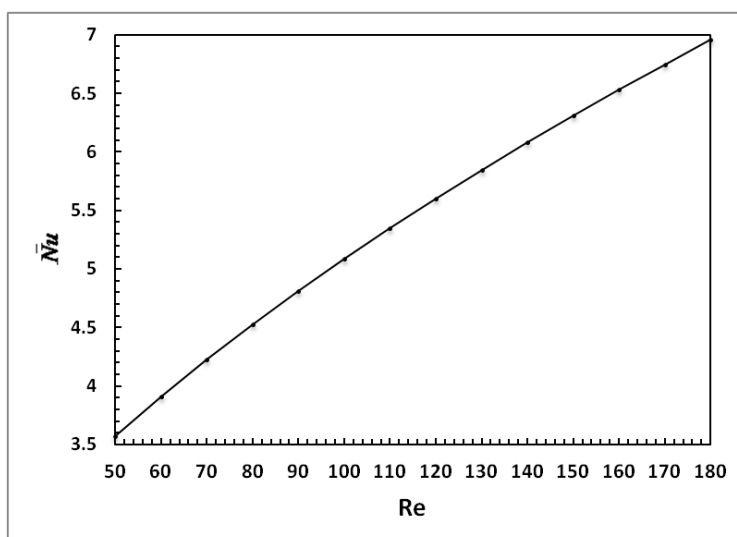Figure 11: Time history of Nusselt number for Re = 100 and 150

Figure 12: Variation of time-averaged Nusselt number with Reynolds number.

V. CONCLUSION

In the present study, unsteady (periodic) flow and forced convection has been simulated for the range of condition: Reynolds number = 50 to 180 (in the steps of 10) in an unconfined flow configuration. The present results are in excellent agreement with the reported experimental and numerical results. Time history profiles of drag coefficient, lift coefficient and Nusselt number are presented for the range of conditions as $50 \leq Re \leq 180$.

Flow pattern is presented via instantaneous streamline, vorticity magnitude, velocity magnitude and pressure profiles across the circular cylinder. As the Reynolds number increases the drag coefficient decreases and the shedding frequency increases; however, the rms drag and rms lift coefficients increase with Reynolds number. The detailed temperature fields near the obstacle are presented by instantaneous profiles of isotherms. The temporal variation of the average Nusselt number is presented. The time averaged Nusselt number increases with increasing value of the Reynolds number for the fixed value of the Prandtl number of 0.7. Finally, simple correlation for time-averaged drag coefficient and time average Nusselt number as a function of Reynolds number are obtained for the range of conditions covered in this study.

Nomenclature

C_D drag coefficient $(= 2F_D / \rho U_\infty^2)$

$\bar{C_D}$ time-averaged drag coefficient

C_{DF} friction drag coefficient

C_{DP} pressure drag coefficient

C_{Drms} rms value of drag coefficient

C_L lift coefficient $(= 2F_L / \rho U_\infty^2)$

C_{LF} friction lift coefficient

C_{LP} pressure lift coefficient

C_{Lrms} rms value of lift coefficient

D_∞ diameter of outer boundary, m

d diameter of a circular cylinder, m

F_D drag force on the cylinder, N/m

F_L lift force on the cylinder, N/m

f vortex shedding frequency $(= s^{-1})$

p pressure $(= p^{'} /(\rho U_\infty^2))$

Re   Reynolds number $(= \rho U_\infty d / \mu)$

St Strouhal number $(= fd / U_\infty)$

t time $[= t^* /(d / U_\infty)]$

V_x component of the velocity in the x-direction $(= V_x^{'} / U_\infty)$

U_∞ uniform velocity of the fluid at the inlet, m s^{-1}

V_y component of the velocity in the y-direction $(= V_y^{'} / U_\infty)$

C_p specific heat of the fluid, J/kg K

h   local convective heat transfer coefficient, W/m^2 K

$\bar{h}$ average convective heat transfer coefficient, W/m2 K

k   thermal conductivity of the fluid, W/m K

n   cylinder surface normal direction

Nu   local Nusselt number $(= hd / k)$

$\overline{Nu}$ average Nusselt number $(= h\, d / k)$

T_∞ temperature of the fluid at the inlet, K

T   temperature $[T = (T^* - T_\infty)/(T_w^* - T_\infty)]$

T_w^* constant wall temperature at the surface of the cylinder

Greek symbols

δ size of the control volume near the cylinder, m

μ viscosity of the fluid, kg m^{-1} s^{-1}

ρ density of the fluid, kg m^{-3}

Subscripts
∞   inlet condition
w   surface of the cylinder
Superscript
*   dimensional variable

REFERENCES

[1.]   Ahmad, R.A., 1996, Steady-state numerical solution of the Navier-Stokes and energy equations around a horizontal cylinder at moderate Reynolds numbers from 100 to 500, Heat Transfer Eng., 17: 31–81.

[2.]   Amit Dhiman, Ravi Golani, 2010, Heat Transfer from a Circular Cylinder in the Unsteady Flow Regime, Proceedings of the 20th National and 9th International ISHMT-ASME Heat and Mass Transfer Conference

[3.]   Amit Dhiman, Mudassir Hasan, 2010, CFD Analysis of the Steady Flow Across a Tapered Trapezoidal Cylinder, Lecture Notes in Engineering & Computer Science, 2184 (1), 1094 – 1096.

[4.]   Amit Kumar Dhiman, Neha Sharma, Surendra Kumar, 2012, Wall effects on the cross-buoyancy around a square cylinder in the steady regime, Brazilian Journal of Chemical Engineering, 29 (2), 253 - 264.

[5.]   Baranyi, L., 2003. Computation of unsteady momentum and heat transfer from a fixed circular cylinder in laminar flow, J. Computational Applied Mechanics, 4: 13 - 25.

[6.]   Braza, M., Chassaing, P., Haminh, H, 1986. Numerical study and physical analysis of the pressure and velocity fields in the near wake of a circular cylinder. J. Fluid Mechanics, 165: 79-130.

[7.]   Chhabra, R. P. and Richardson, J. F., 1999, Non- Newtonian Flow in the Process Industries, Butterworth-Heinemann, Oxford.

[8.]   Eckert E. R. G. and Soehngen E., 1952, Distribution of heat transfer coefficient around circular cylinder in cross flow at Reynolds numbers from 20 to 500. Trans. ASME, **74**, pp. 343 – 347.

[9.]   Isaev, S. A., Leontiev, A. I., Kudryavtsev, N. A., Baranova, T. A., Lysenko, D. A., 2005. Numerical simulation of unsteady state heat transfer under conditions of laminar transverse flow past a circular cylinder, High Temperature, 43 : 746 – 759.

[10.]   Knudsen, J. D. and Katz, D. L., 1958. Fluid Dynamics and Heat Transfer. McGraw Hill, New York.

[11.]   Lange, C. F., Durst F., Breuer M., 1998. Momentum and heat transfer from cylinders in laminar cross flow at $10^{-4} \leq Re \leq 200$, Int. J. Heat Mass Transfer, 41: 3409 - 3430.

[12.]   Lee, T., Budwig, R., 1991. A study of aspect ratio on vortex shedding behind circular cylinders, Physics of Fluids, 3: 310 - 315.

[13.]   Li, J., Cambarel, A., Donneaud, M., Martin, R., 1991. Numerical study of laminar flow past one and two cylinders, Computers Fluids, 19: 155 - 170.

[14.]   Morgan, V. T., 1975. The overall convective heat transfer from smooth circular cylinders, Adv. Heat Transfer, **11**, 199–264.

[15.]   Mittal, S., 2005. Excitation of shear layer instability in flow past a cylinder at low Reynolds number, Int. J. Numerical Methods Fluids, 49: 1147–1167.

[16.]   Mahir, N. and Altac, Z., 2008. Numerical investigation of convective heat transfer in unsteady flow past two cylinders in tandem arrangements, Int. J. Heat Fluid Flow, **29**, pp. 1309–1318.

[17.]   Norberg, C., 2003. Fluctuating lift on a circular cylinder: review and new measurements, J. Fluids Structures, 17: 57 – 96.

[18.]   Nakamura H. and Igarashi T., 2004. Variation of Nusselt number with flow regimes behind a circular cylinder for Reynolds numbers from 70 to 30000, Int. J. Heat and Mass Transfer, **47** (23), pp. 5169 –5173.

[19.]   Neha Sharma, Amit K. Dhiman, Surendra Kumar, 2012, Mixed convection flow and heat transfer across a square cylinder under the influence of aiding buoyancy at low Reynolds numbers,,International Journal of Heat & Mass Transfer, 55, 2601 - 2614.

[20.]   N. S. K. Chaitanya, A. K. Dhiman, 2012, Non-Newtonian power-law flow and heat transfer across a pair of side-by-side circular cylinders, International Journal of Heat & Mass Transfer, 55 (21 - 22) 5941 - 5958.

[21.]   S. Srikanth, A. K. Dhiman, S. Bijjam, 2010, Confined Flow and Heat Transfer Across a Triangular Cylinder in a Channel, International Journal of Thermal Sciences, 49, pp. 2191 - 2200.

[22.]   Patanana,V.K., Bharati, R.P., Chhabra, R.P., (2009). Two-dimensional unsteady flow of power-law fluids over a cylinder, Chemical Engineering Science, 64, pp.2978-2999.

[23.]   Posdziech, O., Grundmann, R.,2007 A systematic approach to the numerical calculation of fundamental quantities of the two-dimensional flow over a circular cylinder, J. Fluids Structures, 23 : 479 – 499

[24.]   Rajani, B. N., Kandasamy, A., Majumdar, S., 2008. Numerical simulation of laminar flow past a circular cylinder, Applied Mathematical Modelling, 33: 1228 - 1247.

[25.]   Sarma T. S. and Sukhatme S. P., 1977, Local heat transfer from a horizontal cylinder to air in crossflow: influence of free convection and free stream turbulence, Int. J. Heat Mass Transfer, **20** (1), pp. 51 – 56.

[26.]   Shi, J.-M., Gerlach, D., Breuer, M., Biswas, G. and Durst F., 2004. Heating effect on steady and unsteady horizontal laminar flow of air past a circular cylinder, Phys. Fluids **16** pp. 4331 – 4345.

[27.]   Sivakumar, P., Bharti, R. P., Chhabra, R.P., 2007. Steady flow of power-law fluids across an unconfined elliptical cylinder, Chem. Engng. Sci., 62, pp.1682 – 1702.

[28.]   S. Srikanth, A. K. Dhiman, S. Bijjam, 2010, Confined Flow and Heat Transfer Across a Triangular Cylinder in a Channel, International Journal of Thermal Sciences, 49,pp. 2191 - 2200.

[29.]   Williamson, C.H.K., 1988. Defining a universal and continuous Strouhal-Reynolds number relationship for the laminar vortex shedding of a circular cylinder, Physics Fluids, 10 : 2742 - 2744.

[30.]   Zhuauskas, A., 1972. Heat transfer from tubes in cross-flow. In: Harnett, J.P., Irwine, T.F. (Eds.), Advances in Heat Transfer, **8**. Academic Press, New York.

[31.]   Zdravkovich, M. M., 1997. Flow Around Circular Cylinders: Fundamentals, Oxford University Press, New York, vol. 1.

[32.]   Zdravkovich, M. M., 2003. Flow Around Circular Cylinders: Fundamentals, Oxford University Press, New York, vol. 2.